Skeletal Radiol (1995) 24:331–336

Skeletal Radiology

Role of technetium-99m pertechnetate scintigraphy in the management of extra-abdominal fibromatosis

Shoji Terui[1], Takashi Terauchi[1], Hiroyuki Abe[1], Yukio Muramatsu[2], Hisatoshi Fukuma[3], Yasuo Beppu[3], Ryohei Yokoyama[3]

[1] Division of Nuclear Medicine, National Cancer Center Hospital, Tokyo, Japan
[2] Division of Diagnostic Radiology, National Cancer Center Hospital, Tokyo, Japan
[3] Division of Orthopedics, National Cancer Center Hospital, Tokyo, Japan

Abstract. The purpose of this study was to investigate technetium-99m pertechnetate (Tc-99m) as a tumor-scanning agent in patients with extra-abdominal fibromatosis, and to establish the sensitivity of this type of scintigraphy. Eleven patients with extra-abdominal fibromatosis were studied: all but one having postsurgical recurrences. Of the 11 patients, diagnosed histologically, 5 underwent repeated Tc-99m scintigraphic follow-up examinations. The injected 370 MBq Tc-99m gave us an early scintigram within 10 min and a delayed one 2 h later. For adequate comparison, the region of interest (ROI) of the scintigram was placed over the tumor. The tumor-to-background (T/BG) count ratio was computed. Extra-abdominal fibromatoses, even recurrences, were demonstrated scintigraphically in both the early and the delayed phase, in all 11 patients. The average T/BG ratio was 2.11 in the early scintigram and 2.15 in the delayed one. The sensitivity and the specificity were both 100%. Tc-99m scintigraphy has proved useful in detecting extra-abdominal fibromatoses and in the follow-up of patients.

Key words: Diagnosis – Scintigraphy – Soft tissue tumor – Extra-abdominal fibromatosis – Technetium-99m

Extra-abdominal fibromatosis is a benign tumor but it is locally aggressive and recurrent [1–9]. Diagnosing local recurrence of this tumor is a great problem, since no really adequate imaging procedure exists for it. The purpose of the present study was to investigate scintigraphy using technetium-99m pertechnetate (Tc-99m) as a scanning technique in patients with this tumor, and to determine its effectiveness [10].

Correspondence to: S. Terui, M.D., Division of Nuclear Medicine, National Cancer Center Hospital, 5-1-1 Tsukiji, Chuo-ku, Tokyo 104, Japan

Materials and methods

From March 1985 to May 1993 (a period of 8 years and 2 months), 11 patients with extra-abdominal fibromatosis were studied with Tc-99m scintigraphy. There were three male and eight female patients, with an average age of 27 years (range 14–43 years). Histological diagnoses were determined by R.Y. (a consultant to the Bone and Soft Tissue Tumor Pathology Section of the Japanese Orthopedic Society) from surgical and/or biopsy specimens stained with hematoxylin and eosin. In addition to the routine pathologic examination, both the vascularity and the cellularity of the tumors were quantified using Yokoyama's method [9]. Briefly, the vascularity was quantified as follows. The number of slit-like blood vessels less than 20 μm in caliber within an ocular micrometer grid (2.5×2.5 mm) was counted under low magnification (×40) with a light microscope. Vascularity of the tumor tissue was divided into three categories based on the number of slit-like blood vessels per 6.25 mm^2 (2.5×2.5 mm): low (less than 9 vessels), moderate (9–15 vessels), or high (more than 15 vessels). In the case of huge tumors, a mixed type of vascularity was observed, part moderate, part high. We classified this as moderate-high vascularity.

The cellularity of the tumor was also divided into three categories based on the number of fibroblastic cells, again low, moderate, and high, and again we classified a mixed type of cellularity as moderate-high cellularity.

Magnetic resonance imaging (MRI) was performed in only six patients and showed eight lesions. MRI was performed using a 1.5-T (MRT 200FX Toshiba, Tokyo) superconducting magnetic system and the multislice conventional spin-echo technique. Both T1-weighted images (TR/TE: 600/15) and T2-weighted images (TR/TE): 2000/80) were obtained. The signal intensity of the tumor on T1- and T2-weighted images was graded relative to the intensities of muscle and fat. These MR images were evaluated by Y.M. in a retrospective study without knowledge of the scintigram results.

Tumor size and number were determined clinically and/or by examination of the specimens. Of the 11 patients, one presented with a tumor without previous treatment while the other 10 presented with a tumor that had recurred locally after one to several episodes of surgical treatment. Five out of 11 patients underwent consecutive scintigraphic follow-up studies using Tc-99m. A total of 22 examinations were carried out, from a minimum of twice to a maximum of five times per patient according to the characteristics of each case.

Scintigraphy was performed in the following way. A dose of 10 mCi (370 MBq) Tc-99m pertechnetate was administered intrave-

nously and scintigraphic images were recorded twice, the early scintigram 5–10 min after the injection, the delayed scintigram 2–3 h later, in order to evaluate the tumor vacularity. The collimator used was of the low-energy, parallel-hole type, and images were acquired with a 64×64 matrix for 5 min per view in each scintigram. The early scintigram was then used for a whole-body study. The early and delayed scintigrams were compared in regard to the uptake of Tc-99m in the tumor. For a final judgement on the Tc-99m uptake in a tumor, we relied, as is our practice, on the delayed scintigram (to exclude the effect of vascularity). Scintigraphically, our follow-up assessments were based on the following conclusions: (1) if there was no Tc-99m uptake by the tumor after treatment, this indicated complete remission; (2) if there was no significant change in uptake on the scintigram, this indicated tumor persistence.

For the quantitative evaluation, the counts of the image data of the spot images in a 64×64 matrix of the early and the delayed scintigrams were stored for 5 min per image in a data analysis computer. Tc-99m accumulates in the tumor and can be recorded on the scintigram. We considered two regions of interest (ROI) assigned to each image; first, over the tumor area, and, second, over the normal soft tissue as the background. The ROI of the background for both the early and the delayed scintigram remained the same. For each ROI, the average counts per pixel were determined by computer.

The tumor-to-background count ratio was determined by dividing the average per pixel counts of the tumor by the counts of the background. Finally, for statistical reasons, we compared the tumor-to-background tissue ratios (T/BG) of both the early and the delayed scintigram.

Results

From the initial scintigrams, 20 tumors were identified in the 11 patients (Table 1). These tumors varied in size as measured clinically and/or by specimen measurement, ranging from 0.8 to 25 cm (mean 5.2 cm). Five (45.5%) patients had a single lesion, 3 (27.3%) had two lesions of the same type, and the remaining three each had three lesions. All of the 20 tumors were revealed as hot spots on the Tc-99m scintigram and all presented clear images; Tc-99m uptake in the tumor was registered in both the early and the delayed scintigrams (Figs. 1–3) and proved greater than the related background activity.

There were two patterns of Tc-99m distribution in the tumors in the early scintigrams. In 7 of the 11 patients an even uptake in the tumor was shown in both the early and the delayed scintigram, and the size of the accumulation did not change. In the other four patients a slight difference in uptake pattern was shown between the early and the delayed scintigrams: on the early scintigrams there was a patchy, uneven uptake in the tumors (Figs. 1B, 2A, 3A), whereas on the delayed scintigrams these accumulations in the tumors extended diffusely to the outer side and seemed to grow in size, although the margin of the accumulation still remained remarkably well defined (Figs. 1C, 2B, 3B).

The histological diagnoses and tumor MR signal intensities in the 11 patients are summarized in Table 1: high vascularity in 8 cases, moderate vascularity in 2, and moderate-high vascularity in 1. As to the cellularity, this was high in 4 cases, moderate-high in 1, and moderate in 6 cases.

MR images detected all eight tumors. On T1-weighted images, the predominant signal intensity was isointense to skeletal muscle. On T2-weighted images, the

Table 1. Results of Tc-99m pertechnetate scintigraphy in 11 patients with extra-abdominal fibromatosis

Case	Sex/age (years)	Location	No. of Tumors	Size (cm)	Uptake pattern on Tc-99m scintigram		Pathology		MRI findings		Follow-up Period[a] (years)	Prognosis
					Early	Delayed	Vascularity	Cellularity	T1	T2		
1.	M/25	Chest wall	1	7×5	Even	Even, same size	High	Moderate	NT	NT	4.7	AWD
2.	F/37	Thigh	2	4.1×2.2	Uneven	Fused, enlarged	High	High	NT	NT	4.8	NED
3.	F/14	Buttock, thigh	2	9×9 2.5×2.5	Uneven	Fused, enlarged	High	Moderate	Iso. Iso.	High & low[b] Iso.	2.1	AWD
4.	F/24	Back	1	2.5×2	Even	Even, same size	High	Moderate	NT	NT	4.3	NED
5.	F/30	Hand	3	3.4×1.4	Even	Even, same size	High	High	NT	NT	2.1	NED
6.	M/20	Back	2	8×5.6	Even	Even, same size	Moderate	Moderate	NT	NT	4.3	NED
7.	F/20	Lower leg	3	6×4.5	Uneven	Fused, enlarged	High	High	Iso. Iso.	High & low Iso.	4.0	NED
8.	M/43	Buttock	1	4.5×4.5	Even	Even, same size	High	High	Iso.	High & low	2.8	NED
9.	F/27	Shoulder	1	6×6.5	Even	Even, same size	Moderate	Moderate	Iso.	High & low	2.7	NED
10.	F/32	Thigh	1	3×2.5	Even	Even, same size	High	Moderate	Iso.	High & low	2.0	NED
11.	F/24	Buttock, thigh	3	25×12	Uneven	Fused, enlarged	Moderate high	Moderate high	Iso.	High & low	6.4	AWD

[a] Disease-free or inactive period from last recurrence or operation
[b] High and low intensity
NT, Not tested; Iso., isointensity; AWD; alive with disease; NED, no evidence of disease

Table 2. Diagnostic reliability of Tc-99m pertechnetate scintigraphy for detection of extra-abdominal fibromatosis

Number of studies		22
Number of correct studies:	true positive	18
	true negative	4
Number of incorrect studies:	false positive	0
	false negative	0
Positive predictive value (%)		100
Negative predictive value (%)		100
Sensitivity (%)		100
Specificity (%)		100
Diagnostic accuracy (%)		100

Table 3. Average tumor-to-background count ratio (T/BG) on Tc-99m pertechnetate scintigrams of extra-abdominal fibromatosis

	No. of studies	T/BG ratio			
		Average	Minimum	Maximum	SD
Early scintigram	22	2.11	0.86	3.45	1.50
Delayed scintigram	22	2.15	1.12	4.03	0.9

signal intensity was inhomogeneous in six tumors; the other two showed the same intensity as skeletal muscle. Inhomogeneous signal intensity reflected inhomogeneity of the number of collagen fibers and of the extent of cellularity. Less collagenous, hypercellular areas corresponded to those with higher intensity on T2-weighted MR images, whereas collagenous, hypocellular portions were represented by lower intensity. In hypercellular areas, collagen fibres were loosely textured, occasionally undergoing myxoid change.

Comparing the scintigrams with the MR images, a strong uptake in the early scintigram corresponded to both the rich cellularity of the tumor and its vascularity. In the delayed scintigram, the whole tumor, even the peripheral hypocellular collagenous areas, was demonstrated (Fig. 1A–E).

The diagnostic effectiveness of the Tc-99m scintigram, based on the 22 examinations, is summarized in Table 2. In both the primary and the recurrent cases, the Tc-99m scintigram showed no false positive results. Thus both sensitivity and specificity rated 100%.

Five out of 11 patients underwent a total of 16 consecutive scintigraphic follow-up examinations with Tc-99m. Among these 5 patients, 2 experienced no further recurrence (complete remission) and 3 had residual tumor or developed local recurrence (tumor persistence).

T/BG ratio was calculated from the visualized tumors on the Tc-99m scintigram (Table 3). The T/BG ratio of the Tc-99m scintigram was 2.11 on the early scintigram and 2.15 on the delayed one.

For illustration, three significant medical histories are given below.

Case 7 (Fig. 1) is that of a 20-year-old woman with extra-abdominal fibromatosis of the left posterior thigh which has recurred after surgery. The whole-body scintigram shows two abnormal accumulations; one is a horseshoe-shaped strong uptake in the left posterior thigh and the other a weak uptake in the left leg posteriorly (Fig. 1A). The latter tumor was identified clinically only with the Tc-99m scintigram. Accumulations in the parotid glands, submandibular glands, thyroid glands, stomach, and bladder are normal variants. On the early scintigram, tumors of the left thigh are well defined (Fig. 1B). On the delayed scintigram, the accumulations of the tumors fuse and extend to the margin of the tumor (Fig. 1C). The accumulation thus seems to grow in size, though its margin is still remarkably well defined. On MRI, these tumors are shown as a high intensity area on T2-weighted images (Fig. 1D, E). The tumors were subsequently surgically excised as completely as possible. The post-operative scintigram shows no abnormal accumulations (Fig. 1F). Microscopy of sections from the surgical specimens showed fibroblastic cells and intercellular collagen fibers (Fig. 1G). Both the vascularity and the cellularity were classified as high in this case.

Case 11 (Fig. 2) is an example of a 24-year-old woman with recurrent extra-abdominal fibromatosis of the right posterior thigh. On the posterior view of the early scintigram, huge nodular accumulations are present, consistent with the clinically palpated tumors, and these margins are well defined (Fig. 2A). On the delayed scintigram, accumulation extends diffusely to the surrounding tissue and its uptake becomes evenly spread (Fig. 2B). The margin that has emerged is well defined. We diagnosed this margin on the delayed scintigram as a real tumor extension.

Case 5 (Fig. 3) is the case of a 30-year-old woman with recurrent extra-abdominal fibromatosis on the back of the left had. She had undergone surgery 2 years before. Three tumors measuring 34×17 mm, 22×12 mm, and 17×14 mm respectively were still palpable in the hand. The early scintigram shows a well-defined nodular accumulation consistent with the palpable tumors (Fig. 3A). On the delayed scintigram, the accumulation extends diffusely and the lower part of the margin reaches the wrist (Fig. 3B). We concluded that the tumors were now actively growing.

Figure 3C shows the early scintigram taken 42 months after Fig. 3A and B: it is similar to the scintigram obtained 42 months earlier. Figure 3D shows the same appearance, although it has been obtained by a new delayed scintigram. The tumor appears to be inactive.

Discussion

Extra-abdominal fibromatosis is not only a rare but also a unique lesion which tends to recur in spite of its harmless microscopic appearance [1–9]. The recurrence rate as reported so far varies from 25% to 77% [3–9, 11–13]. A far greater problem than diagnosing the primary tumor is accurately judging the extent of a locally recurrent extra-abdominal fibromatosis, because a part of the recurrent tumor is often confused with operative scar tissue.

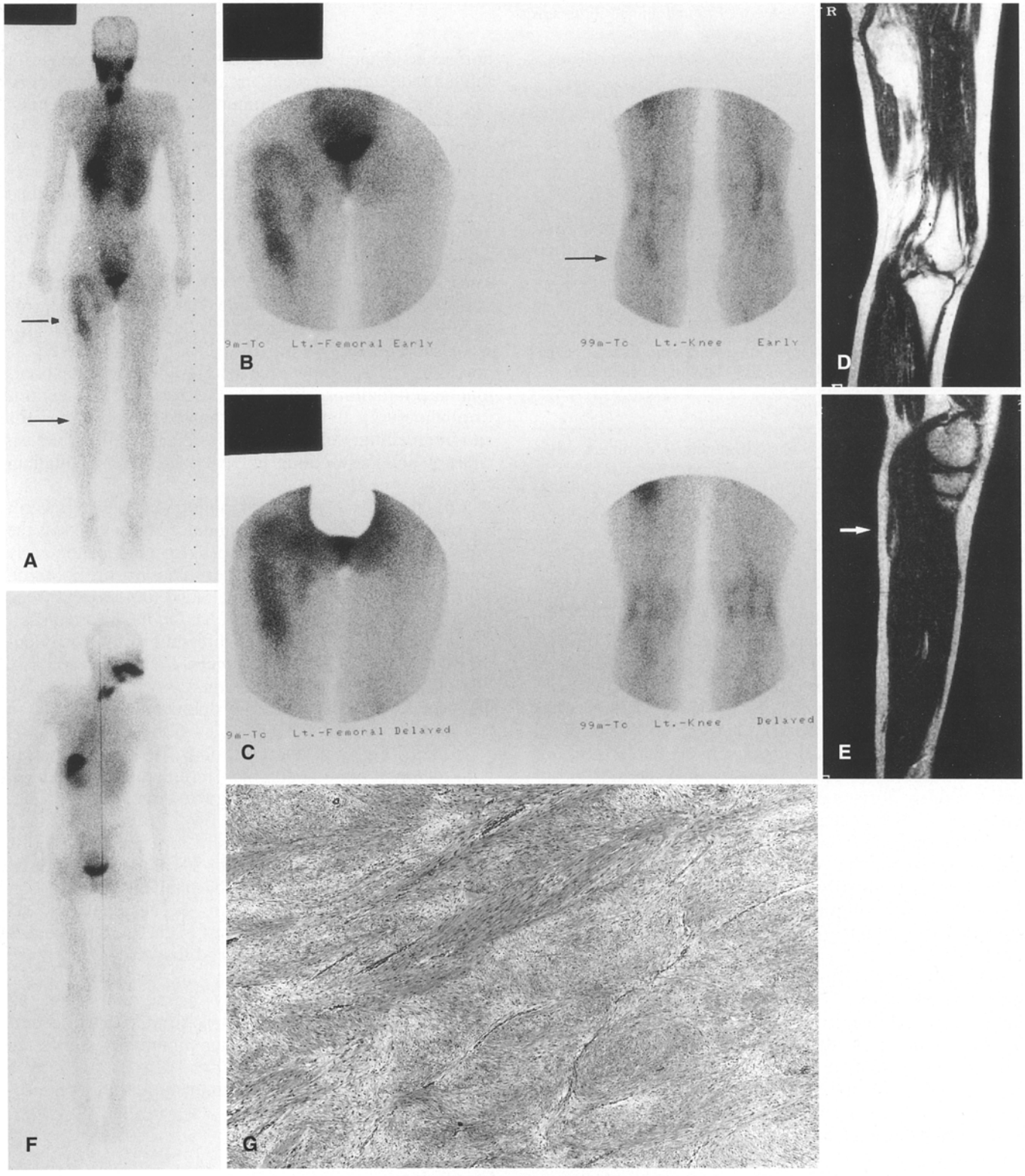

Fig. 1A–G. Case 7: a 20-year-old woman with an extra-abdominal fibromatosis of the left posterior thigh which has recurred after surgery. **A** Whole-body posterior scintigram obtained at 10 min after administration of Tc-99m pertechnetate. Two abnormal accumulations are in the left posterior thigh and the left posterior leg (*arrows*). **B** Spot images of the early scintigram demonstrate uneven uptake of Tc-99m in the left posterior thigh (*left*) and even uptake in the left posterior leg (*right, arrow*). **C** Spot images of the delayed scintigram obtained 2 h after administration of Tc-99m pertechnetate. The uptake of Tc-99m in the left posterior thigh (*left*) and the left posterior leg (*right*) have fused and extended to the outside. The accumulation seems to have grown in size, though its margin is still remarkably well defined. **D** T2-weighted MR image of the thigh shows a well-defined soft tissue mass. Signal intensity is both hyperintense and isointense to skeletal muscle. **E** T2-weighted image of the lower limb shows a well-defined soft tissue mass (*arrow*). Signal intensity is isointense to skeletal muscle. **F** Whole-body posterior scintigram obtained at 10 min after administration of Tc-99m pertechnetate. This is a post-operative study performed 1 year after the surgery and shows no abnormal accumulations. **G** Photomicrograph showing slit-like vessels and spindle-shaped cells composed of sweeping bundles. Both the vascularity and the cellularity are high. (H&E, ×50)

Until the present study, radionuclide scans have not been routinely used in dealing with extra-abdominal fibromatosis [10, 14–20].

Using Tc-99m pertechnetate scintigrams, we were able to visualize and define the extent of extra-abdominal fibromatosis in all 11 patients. The advantage of Tc-99m scintigrams is that they allow one to survey the whole patient as well as to detect recurrent extra-abdominal fibromatosis (Fig. 1A). The mechanism of uptake of Tc-99m in the tumors is unknown at present. Accumulations in the early scintigram most likely depend on both blood flow and the capillary permeability of Tc-99m or active transport through the cell membranes of the tumor cells. The early scintigram is considered to reflect blood-pooling, while no such phenomenon has been observed in the delayed scintigram. The following hypothesis seems to be reasonable: Tc-99m is transported either passively or actively through the cell membrane into the cytoplasm of the active tumor cells. This seems to be confirmed by the T/BG (tumor/background) ratio, which is higher in the delayed scintigram than in the early one (Table 3).

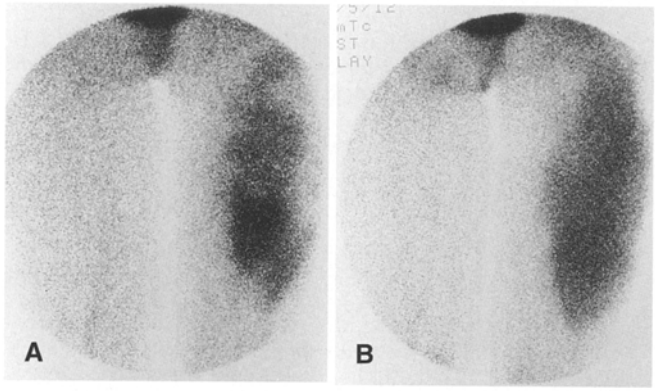

Fig. 2A, B. Case 11: a 24-year-old woman with a recurrent extra-abdominal fibromatosis of the right posterior thigh. **A** Early scintigram of the posterior of the right thigh demonstrates huge nodular accumulations consistent with the clinical findings. The margins of the tumors are well defined. **B** Delayed scintigram taken 3 h after **A**. The accumulation is diffusely extending to the surroundign tissue and its uptake becomes evenly spread. However, the margin is still well defined

Histologically, extra-abdominal fibromatosis consists of spindle-shaped fibroblastic cells accompanying intercellular collagen fibers in sweeping bundles. In addition, other changes may be seen, including myxoid change, focal hemorrhage, and focal inflammation [9, 12]. Hawnaur et al. [21] describe the way MRI reflects the pathological findings; the very low signal intensity of fibrous tissue being predominantly peripheral and the areas with enhancing, intermediate signal intensity being more central.

Our study did not carry out a precise comparison between MRI and Tc-99m scintigraphy, as MRI began to function in our hospital only in July 1989, whereas our clinical study began in 1985. During the period between

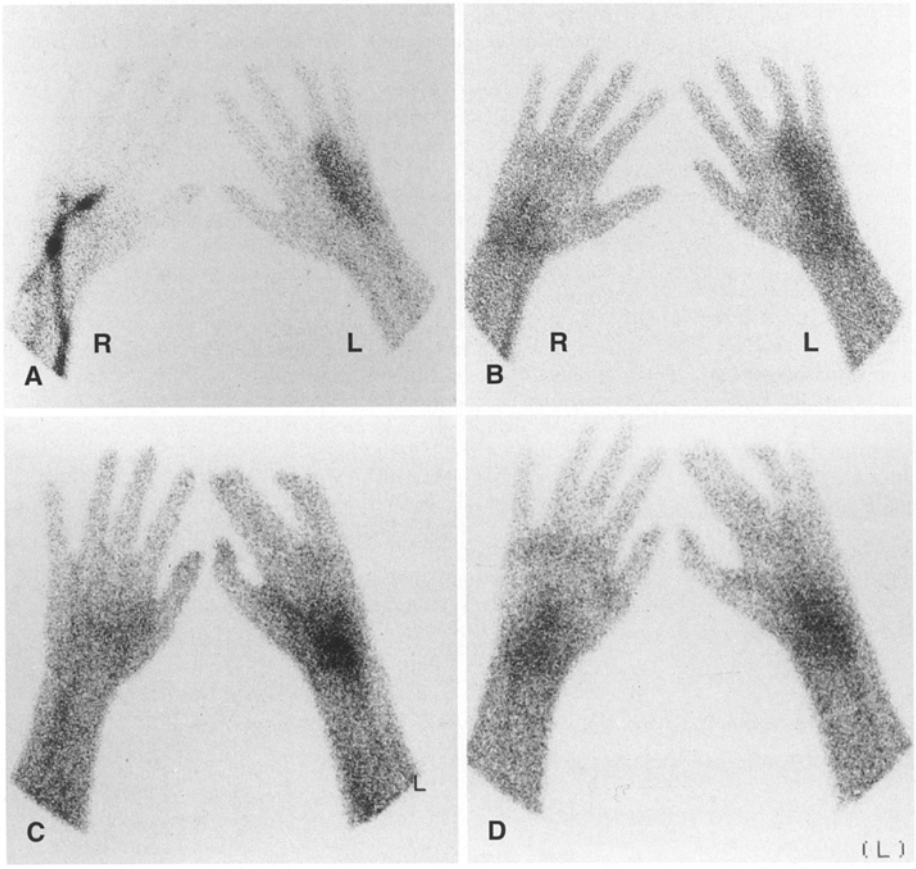

Fig. 3A–D. Case 5: a 30-year-old woman with a recurrent extra-abdominal fibromatosis on the back of the left hand. **A** Early Tc-99m scintigram shows a well-defined nodular accumulation in the back of the left hand. **B** The delayed scintigram shows the accumulation extending diffusely with the lower part of the margin reaching the wrist. **C** Early scintigram taken 42 months after **A** and **B**. It provides the same picture as the earlier delayed scintigram (**B**). **D** The delayed scintigram obtained 3 h after **C**. Compared with **C**, the uptake of Tc-99m did not change and did not spread diffusely

1989 and 1991, we performed MRI examinations without scintigraphy; it is only since 1991 that we have been combining MRI and scintigraphy. This disease being rare, they have been very few patients admitted even to our large hospital, preventing us from acquiring many patients with MRI/scintigraphic correlation.

Although only eight tumors have been examined and their scintigrams compared with MR images, we feel confident in asserting that the strong uptake of the early scintigram corresponds to both the rich cellularity and the vascularity of the tumor, and the fused and extended uptake of the delayed scintigram corresponds to the tumor cells embedded with the collagen fibers. This indicates that the Tc-99m appearances of extra-abdominal fibromatosis correlate well with the histological changes, and the areas of even Tc-99m uptake of the tumor on the delayed scintigram apparently correspond to the tumor extension.

As yet, we do not understand the two types of Tc-99m uptake pattern on the early scintigram. Increased uptake on the delayed scintigram compared with the early scintigram implies that the tumors may be in the actively growing stage. On the other hand, no difference in the distribution of Tc-99m in the tumors between the early and the delayed scintigram suggests that the tumors are either in a nonactive stage or have simply ceased growing (Fig. 3C, D).

MRI is certainly one of the best imaging methods for detecting and identifying the extent of soft tissue disease [9, 21–26]. Tc-99m scintigraphy in conjunction with MRI is clinically truly useful and offers an accessible examination tool in the follow-up of patients suffering from these rare tumors.

Acknowledgement. This research was supported by Daiichi Radiopharmaceutical Lab., Japan.

References

1. Allen PW. The fibromatoses: a clinicopathologic classification based on 140 cases, Part 1. Am J Surg Pathol 1977; 1: 255-270.
2. Dahn I, Jonsson, Lundh G. Desmoid tumors. A series of 33 cases. Acta Chir Scand 1963; 126: 305–314.
3. Das Gupta TK, Brasfield RD, O'Hara J. Extraabdominal desmoids: a clinicopathologic study. Ann Surg 1969; 170: 109–121.
4. Enzinger FM, Shiraki M. Musculo-aponeurotic fibromatosis of the shoulder girdle (extra-abdominal desmoid): analysis of 30 cases followed up for 10 or more years. Cancer 1967; 20: 1131–1140.
5. Hunt RTN, Morgan HC, Ackerman LV. Principles in the management of extra-abdominal desmoids. Cancer 1960; 13: 825–836.
6. Markehede G, Lundgren L, Bjurstam N, et al. Extra-abdominal desmoid tumors. Acta Orthop Scand 1986; 57: 1–7.
7. Musgrove JE, McDonald JR. Extra-abdominal desmoid tumors: their differential diagnosis and treatment. Arch Pathol 1948; 45: 513–540.
8. Rock MG, Pritchard DJ, Reiman HM, et al. Extra-abdominal desmoid tumors. J Bone Joint Surg [Am] 1984; 66: 1369–1374.
9. Yokoyama R, Tsuneyoshi M, Enjoji M, Shinohara N, Masuda S. Extra-abdominal desmoid tumors: correlations between histologic features and biological behavior. Surg Pathol 1989; 2: 29–42.
10. Terui S, Oyamada H, Fukuma H, Beppu Y, Chuuman K. Direct tumor scintigraphy for bone tumors and soft part sarcomas using Tc-99m pertechnetate. Nippon Acta Radiol 1986; 46: P197.
11. Cole NM, Guiss LW. Extra-abdominal desmoid tumors. Arch Surg 1969; 98: 530–533.
12. Enzinger FM, Weiss SW, Soft tissue tumors. St Louis: Mosby, 1983.
13. Ramsey RH. The pathology, diagnosis, and treatment of extra-abdominal desmoid tumors. J Bone Joint Surg [Am] 1955; 37: 1012–1018.
14. Blatt CJ, Hayt DB, Desai M, Freeman LM. Soft tissue sarcoma imaged with technetium-99m pyrophosphate.. N Y State J Med 1977; 77: 2118–2119.
15. Desai A, Eymontt M, Alavi A, Schaffer V, Dalinka MK. Tc-99m MDP uptake in nonosseous lesions. Radiology 1980; 135: 181–184.
16. Kayfman JH, Cedermark BL, Parthasarathy KL, Didolkar MS, Bakshi SP. The values of Ga-67 scintigraphy in soft-tissue sarcoma and chondrosarcoma. Radiology 1977; 123: 131–134.
17. Matsui K, Yamada H, Chiba K, Ito M. Visualization of soft tissue malignancies by using Tc-99m polyphosphate, pyrophosphate and diphosphonate (Tc-99mP). J Nucl Med 1973; 14: 632–633.
18. Ohta H, Endo K, Fujita T, et al. Imaging of soft tissue tumors with Tc(V)-99m dimercaptosuccinic acid: a new tumor-seeking agent. Clin Nucl Med 1984; 9: 568–573.
19. Richman LS, Gumerman LW, Levine G, Sartiano GP, Boggs SS. Localization of Tc-99m polyphosphate in soft tissue malignancies, AJR 1975; 124: 577–582.
20. Rosenthal L. Tc-99m-Methylene diphosphonate concentration in soft tissue malignant fibrous histiocytoma. Clin Nucl Med 1978; 3: 58–61.
21. Hawnaur JM, Jenkins JPR, Isherwood I. Magnetic resonance imaging of musculoaponeurotic fibromatosis. Skeletal Radiol 1990: 19: 509–514.
22. Casillas J, Sais GJ, Greve JI. Imaging of intra- and extraabdominal desmoid tumors. Radiographics 1991; 11: 959–968.
23. Feld R, Burk DL Jr, McCue P, et al. MRI of aggressive fibromatosis: frequent appearance of high signal intensity of T2-weighted images. Magn Reson Imaging 1990; 8: 583–588.
24. Hartman TE, Berquist TH, Fetsch JF. MR imaging of extraabdominal desmoids: differentiation from other neoplasms. Am J Roentgenol 1992; 158: 581–585.
25. Kransdorf MJ, Jelinek JS, Moser RP Jr, et al. Magnetic resonance appearance of fibromatosis. A report of 14 cases and review of the literature. Skeletal Radiol 1990; 19: 495–499.
26. Vanel D, Shapeero LG, De Baere T, et al. MR imaging in the follow-up of malignant and aggressive soft-tissue tumors: results of 511 examinations. Radiology 1994; 190: 263–268.